Supporting Information

Composite gel-polymer electrolyte for high-loading polysulfide cathodes

Li-Ling Chiu[a] and Sheng-Heng Chung[a,b,*]

[a] Department of Materials Science and Engineering, National Cheng Kung University, No. 1, University Road, Tainan City 701

[b] Hierarchical Green-Energy Materials Research Center, National Cheng Kung University, No. 1, University Road, Tainan City 701

*Sheng-Heng Chung: SHChung@gs.ncku.edu.tw

To whom correspondence should be addressed

Supporting Figures

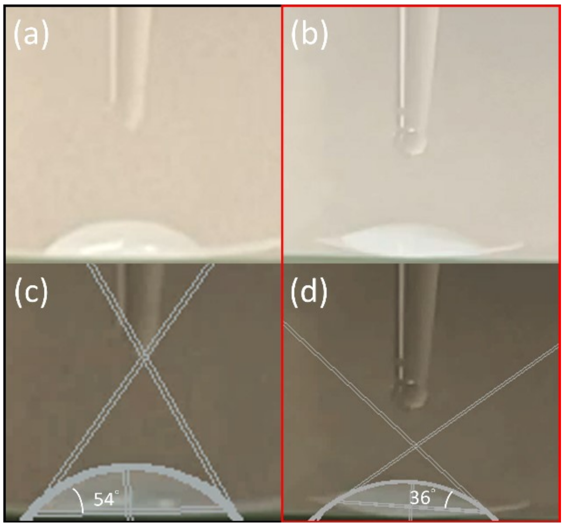

Fig. S1. Electrolyte affinity analysis: the contact angle of (a,c) polypropylene substrate and (b,d) PMMA-based GPE.

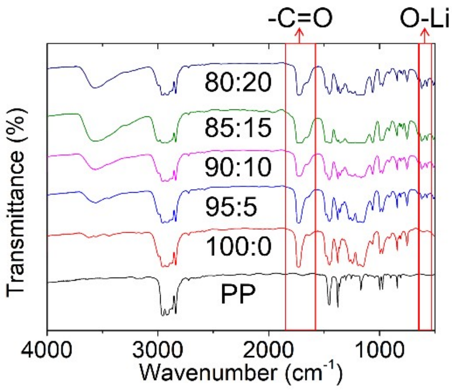

Fig. S2. Fourier-transform infrared (FTIR) spectroscopy of polymethyl methacrylate (PMMA)-based gel-polymer electrolyte (GPE) with different PMMA:LiTFSI ratios of 100:0, 95:5, 90:10, 85:15, and 80:20 wt% and the reference polymeric separator.

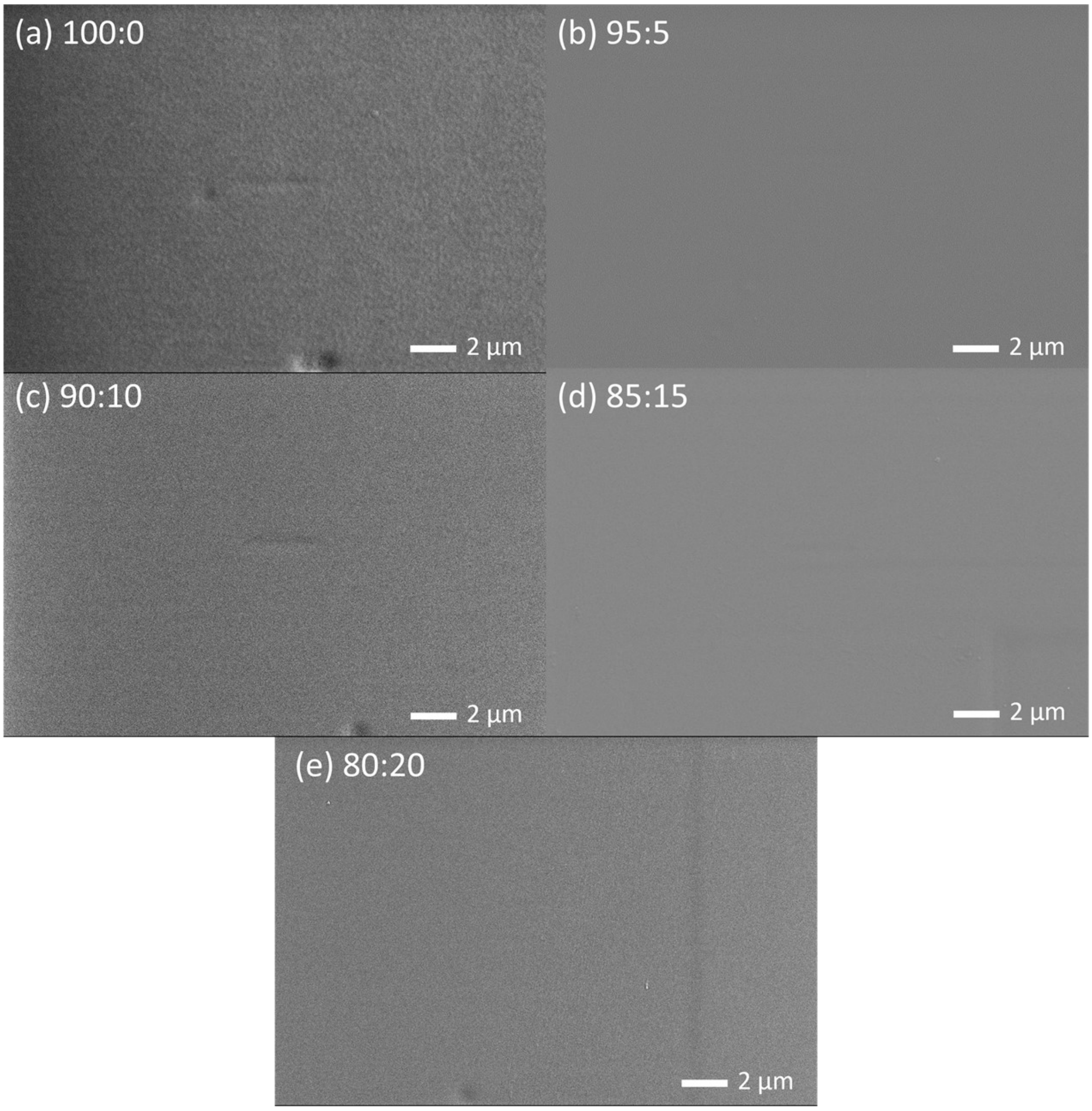

Fig. S3. Morphology analysis of PMMA-based GPE with different PMMA:LiTFSI ratios: (a) 100:0, (b) 95:5, (c) 90:10, (d) 85:15, and (e) 80:20 wt%.

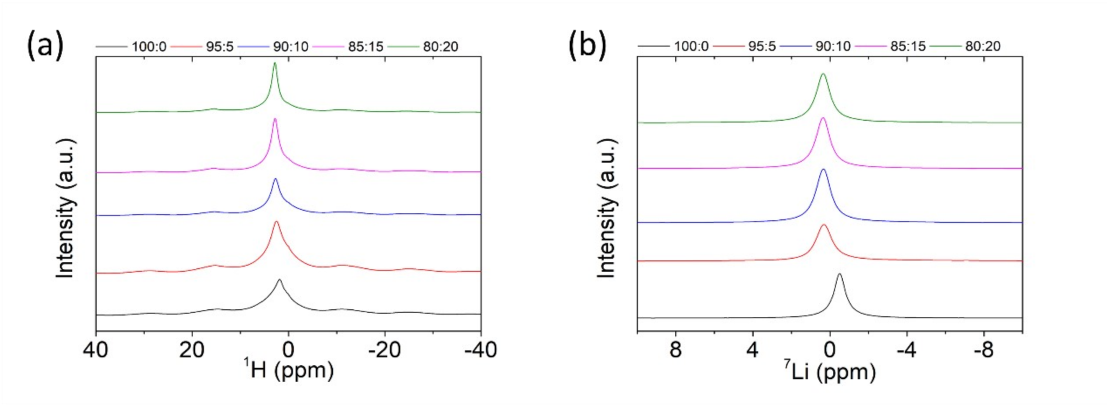

Fig. S4. Solid-state NMR of PMMA-based GPE with different PMMA:LiTFSI ratios of 100:0, 95:5, 90:10, 85:15, and 80:20 wt%: (a) ^{1}H NMR and (b) ^{7}Li NMR.

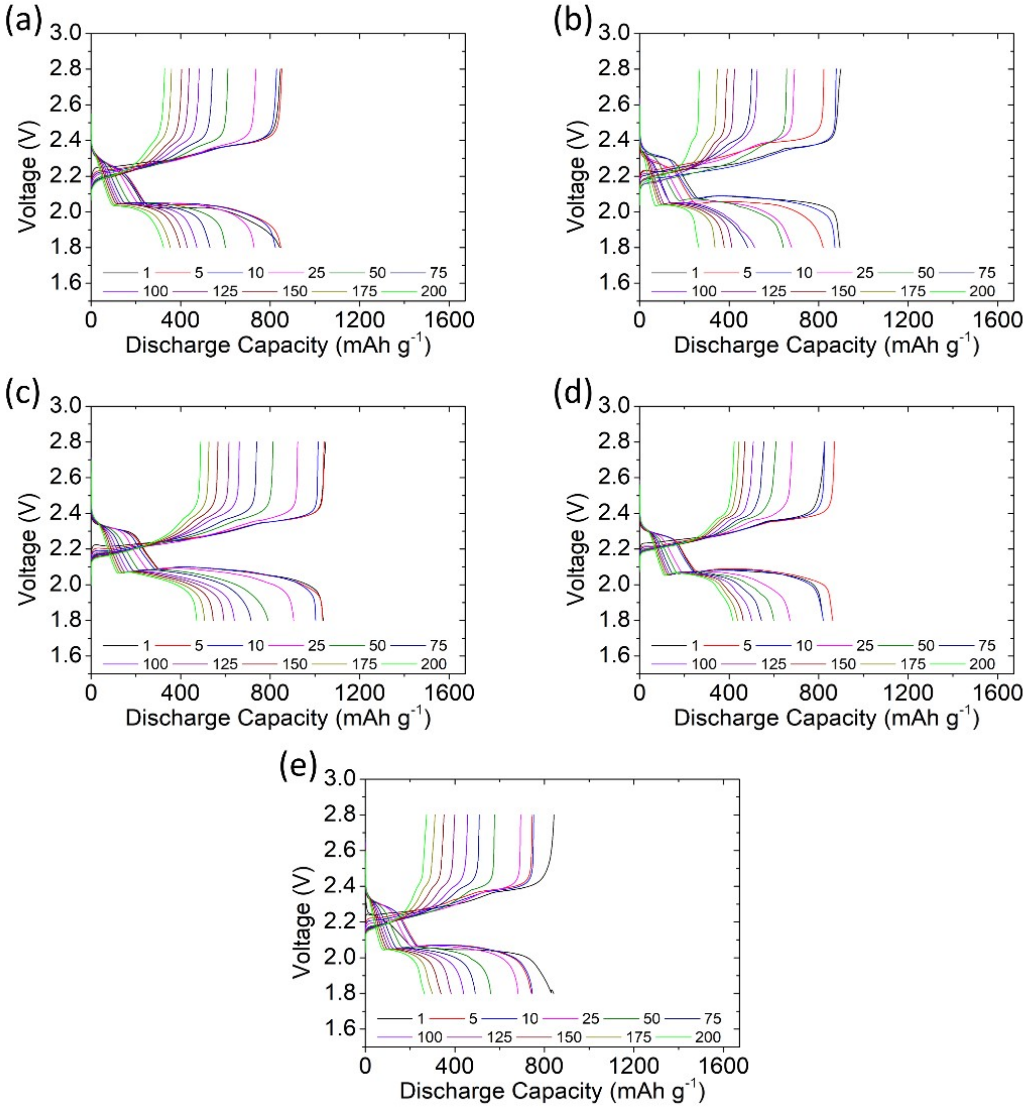

Fig. S5. Discharge/charge curves of high-sulfur-loading polysulfide cathodes with PMMA-based GPE with different PMMA:LiTFSI ratios: (a) 100:0, (b) 95:5, (c) 90:10, (d) 85:15, and (e) 80:20 wt%.

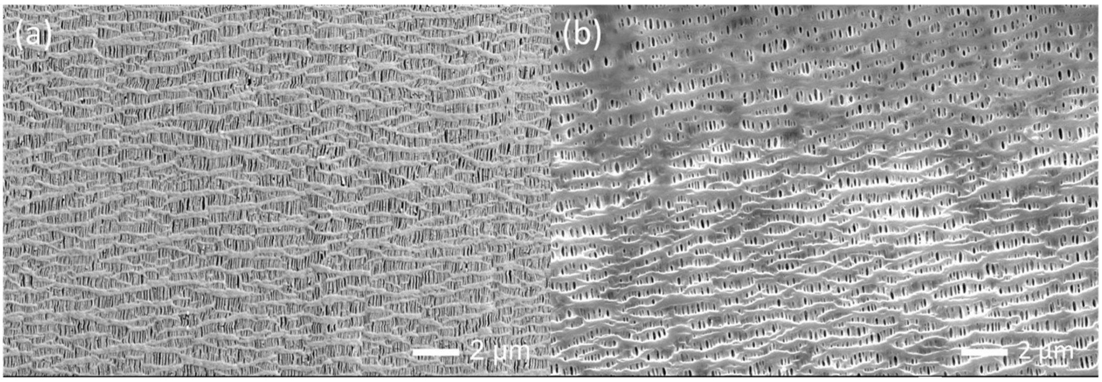

Fig. S6. Microstructural inspection from the anode side of PMMA-based GPE (a) before and (b) after cycling.

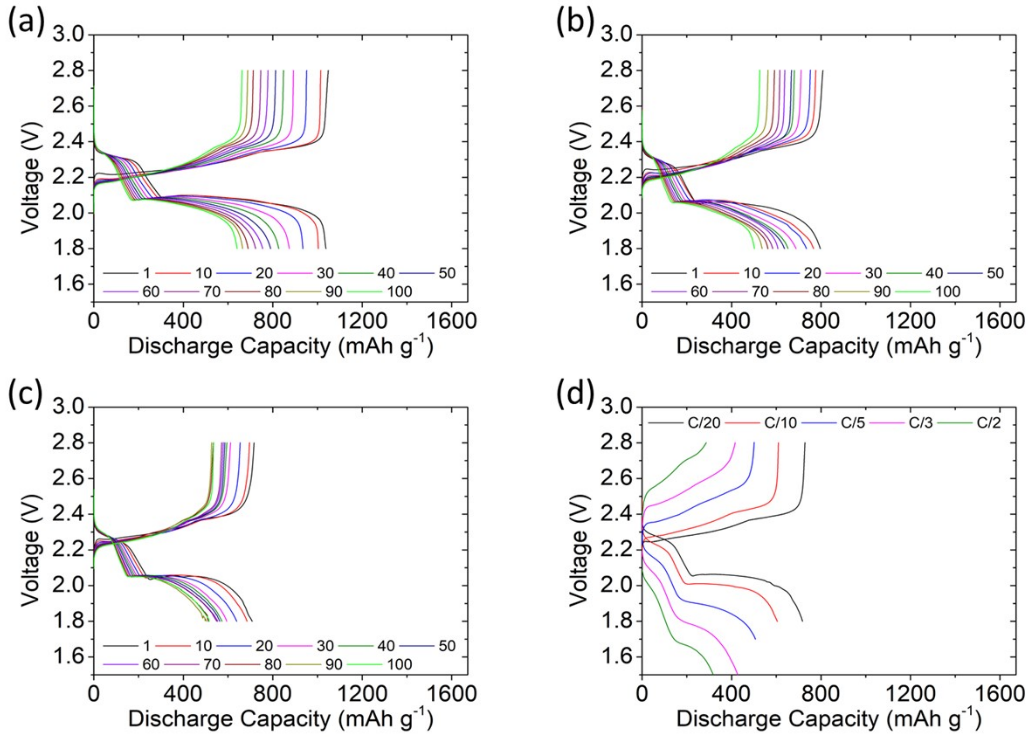

Fig. S7. Discharge/charge curves of high-sulfur-loading polysulfide cathodes with PMMA-based GPE (PMMA:LiTFSI = 90:10 wt%): (a) 4 mg cm^{-2} sulfur, (b) 8 mg cm^{-2} sulfur, and (c) 10 mg cm^{-2} sulfur; and (d) rate capacity of sulfur loading of 10 mg cm^{-2}.

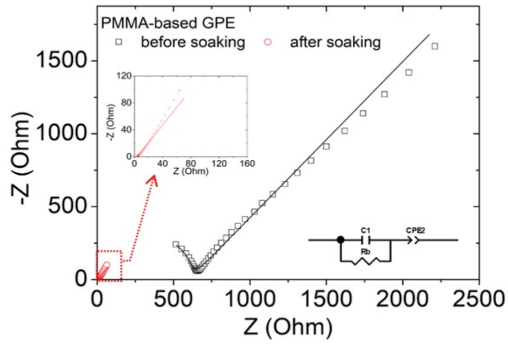

Fig. S8. Ionic conductivities of PMMA-based GPE before and after soaking electrolyte.

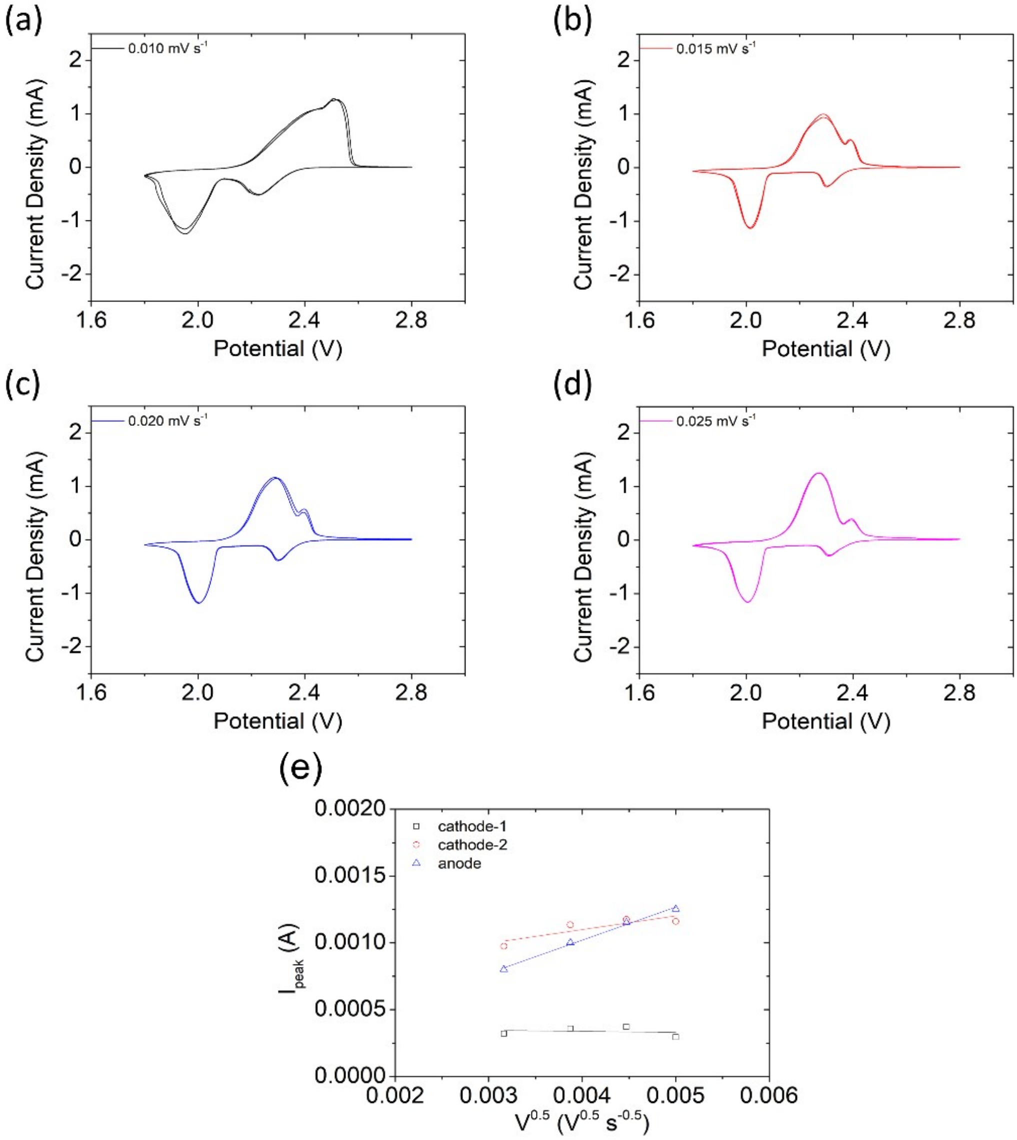

Fig. S9. Cyclic voltammetry (CV) analysis of high-sulfur-loading polysulfide cathodes with 4 mg cm^{-2} sulfur and with PMMA-based GPE (PMMA:LiTFSI = 90:10 wt%) at different scan rates: (a) 0.010 mV s^{-1}, (b) 0.015 mV s^{-1}, (c) 0.020 mV s^{-1}, and (d) 0.025 mV s^{-1} and (e) lithium-ion diffusion coefficient analysis.

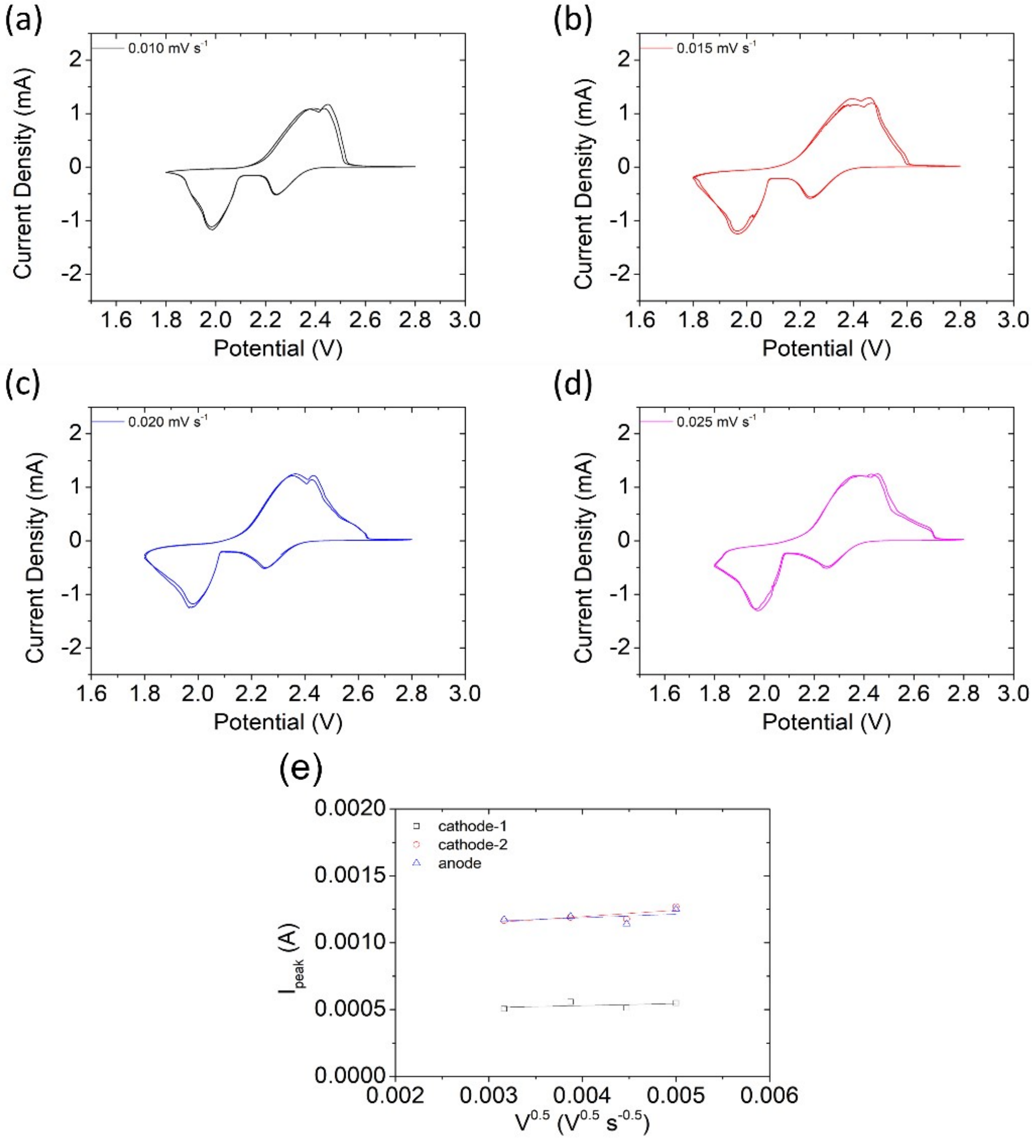

Fig. S10. CV analysis of high-sulfur-loading polysulfide cathodes with 8 mg cm^{-2} sulfur and with PMMA-based GPE (PMMA:LiTFSI = 90:10 wt%) at different scan rates: (a) 0.010 mV s^{-1}, (b) 0.015 mV s^{-1}, (c) 0.020 mV s^{-1}, and (d) 0.025 mV s^{-1} and (e) lithium-ion diffusion coefficient analysis.

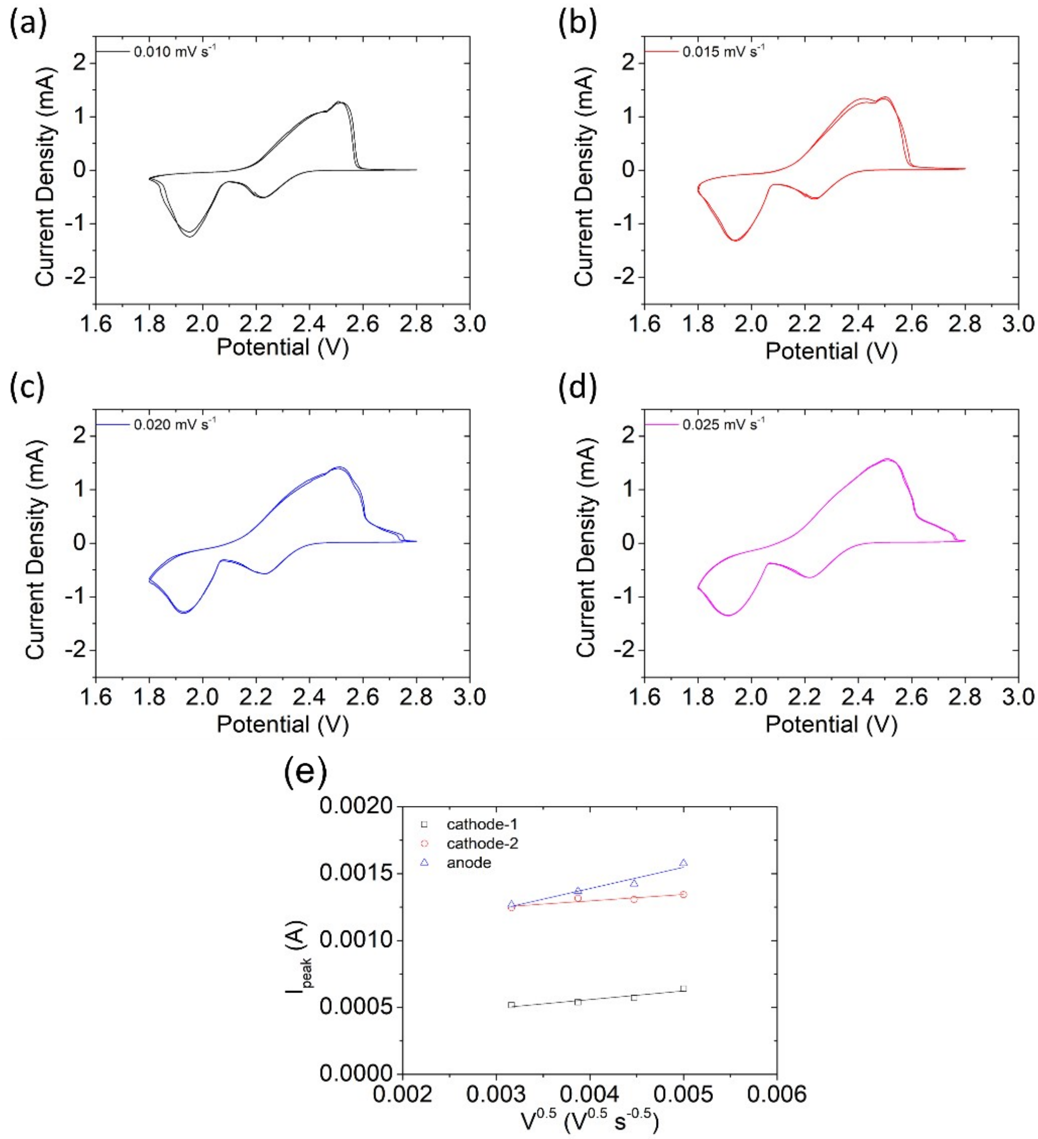

Fig. S11. CV analysis of high-sulfur-loading polysulfide cathodes with 10 mg cm^{-2} sulfur and with PMMA-based GPE (PMMA:LiTFSI = 90:10 wt%) at different scan rates: (a) 0.010 mV s^{-1}, (b) 0.015 mV s^{-1}, (c) 0.020 mV s^{-1}, and (d) 0.025 mV s^{-1} and (e) lithium-ion diffusion coefficient analysis.

Supporting Table

Table S1. Comparative of battery performance and electrochemical abilities with gel-polymer electrolyte in lithium-sulfur batteries.

A	B	C	D	E	F	G	H
2016	60	1.8	PAN/PMMA-electrospun/PETEA	1.43	475.2	3.0	[S1]
2016	56	1.5	PETEA	0.79	296.6	1.7	[S2]
2016	34	1	PVDF/PMMA/PVDF	1.17	399	2.5	[S3]
2017	82	5.2	PVDF/PEO/ZrO_2	4.57	720.8	9.6	[S4]
2017	48	2	PVDF-HFP/LATP	1.8	440.6	3.9	[S5]
2018	70	1	PDA-modified PVDF-based GPE	1.22	850.8	2.6	[S6]
2018	49	1.2	poly(acrylic acid) (PAA)	0.67	275.4	1.4	[S7]
2019	48	1	PMMA/separator/AB	0.99	477.4	2.1	[S8]
2019	49	0.55	PP(Celgard 2400)/PMMA	0.61	539.1	1.3	[S9]
2019	38	1	PVDF/PMMA	0.55	210.4	1.2	[S10]
2019	54	1	PAN/PEO/LATP	0.90	487.9	1.9	[S11]
2019	48	1.2	PVDF-HFP/PETT	0.72	288.5	1.5	[S12]
2020	48	2	PETT-DA, PVDF-HFP	1.41	338.2	3.0	[S13]
2020	64	2	PEGDA/LLZTO	2.40	768.6	5.0	[S14]
2020	65	2	PVDF-HFP/PSD	2.46	798.9	5.2	[S15]

2020	60	1.1	PVDF-HFP	1.1	600	2.3	[S16]
2020	70	2	PVDF/PSPEG	1.89	660.1	4.0	[S17]
2021	70	1	PEI/PEGME	0.94	658	2.0	[S18]
2021	76	6	PEO/LiTFSI	3.82	484.1	8.0	[S19]
2021	60	1.5	PVA-CN or PDXL	1.59	637.8	3.3	[S20]
	73	10	PMMA/LiTFSI	7.10	509.8	15.1	This work

A: Year, B: sulfur content [wt%], C: sulfur loading [mg cm^{-2}], D: polymer, E: areal capacity [mA·h cm^{-2}], F: gravimetric capacity [mA·h g^{-1}], G: energy density [mW·h cm^{-2}], H: references.

Supporting References

S1. M. Liu, H. R. Jiang, Y. X. Ren, D. Zhou, F. Y. Kang and T. S. Zhao, *Electrochim. Acta*, 2016, **213**, 871-878.

S2. M. Liu, D. Zhou, Y.-B. He, Y. Fu, X. Qin, C. Miao, H. Du, B. Li, Q.-H. Yang, Z. Lin, T. S. Zhao and F. Kang, *Nano Energy*, 2016, **22**, 278-289.

S3. W. Yang, W. Yang, J. Feng, Z. Ma and G. Shao, *Electrochim. Acta*, 2016, **210**, 71-78.

S4. S. Gao, K. Wang, R. Wang, M. Jiang, J. Han, T. Gu, S. Cheng and K. Jiang, *J. Mater. Chem. A*, 2017, **5**, 17889-17895.

S5. Y. Xia, X. Wang, X. Xia, R. Xu, S. Zhang, J. Wu, Y. Liang, C. Gu and J. Tu, *Chem. Eur. J.*, 2017, **23**, 15203-15209.

S6. D.-D. Han, S. Liu, Y.-T. Liu, Z. Zhang, G.-R. Li and X.-P. Gao, *J. Mater. Chem. A*, 2018, **6**, 18627-18634.

S7. S. Song, L. Shi, S. Lu, Y. Pang, Y. Wang, M. Zhu, D. Ding and S. Ding, *J. Membr. Sci.*, 2018, **563**, 277-283.

S8. D. Yang, L. He, Y. Liu, W. Yan, S. Liang, Y. Zhu, L. Fu, Y. Chen and Y. Wu, *J. Mater. Chem. A*, 2019, **7**, 13679-13686.

S9. C. Deng, Z. Wang, S. Wang, J. Yu, D. J. Martin, A. K. Nanjundan and Y. Yamauchi, *ACS Appl. Mater. Interfaces*, 2019, **11**, 541-549.

S10. Y. Liu, D. Yang, W. Yan, Q. Huang, Y. Zhu, L. Fu and Y. Wu, *iScience*, 2019, **19**, 316-325.

S11. X. Wang, X. Hao, Y. Xia, Y. Liang, X. Xia and J. Tu, *J. Membr. Sci.*, 2019, **582**, 37-47.

S12. Y. Xia, Y. F. Liang, D. Xie, X. L. Wang, S. Z. Zhang, X. H. Xia, C. D. Gu and J. P. Tu, *Chem. Eng. J.*, 2019, **358**, 1047-1053.

S13. X. Wang, X. Hao, D. Cai, S. Zhang, X. Xia and J. Tu, *Chem. Eng. J.*, 2020, **382**, 122714.

S14. D. Shao, L. Yang, K. Luo, M. Chen, P. Zeng, H. Liu, L. Liu, B. Chang, Z. Luo and X. Wang, *Chem. Eng. J.*, 2020, **389**, 124300.

S15. J.-H. Jiang, A.-B. Wang, W.-K. Wang, Z.-Q. Jin and L.-Z. Fan, *J. Energy Chem.*, 2020, **46**, 114-122.

S16. J. Yu, S. Liu, G. Duan, H. Fang and H. Hou, *Compos. Commun.*, 2020, **19**, 239-245.

S17. Y.-Q. Shen, F.-L. Zeng, X.-Y. Zhou, A.-b. Wang, W.-k. Wang, N.-Y. Yuan and J.-N. Ding, *J. Energy Chem.*, 2020, **48**, 267-276.

S18. T. Zhang, J. Zhang, S. Yang, Y. Li, R. Dong, J. Yuan, Y. Liu, Z. Wu, Y. Song, Y. Zhong, W. Xiang, Y. Chen, B. Zhong and X. Guo, *ACS Appl. Mater. Interfaces*, 2021, **13**, 44497-44508.

S19. L.-L. Chiu and S.-H. Chung, *Polymers*, 2021, **13**, 535.

S20. Y.-J. Yang, R. Wang, J.-X. Xue, F.-Q. Liu, J. Yan, S.-X. Jia, T.-Q. Xiang, H. Huo, J.-J. Zhou and L. Li, *J. Mater. Chem. A*, 2021, **9**, 27390-27397.